Nuclear Materials and Energy 37 (2023) 101540

Contents lists available at ScienceDirect

Nuclear Materials and Energy

journal homepage: www.elsevier.com/locate/nme

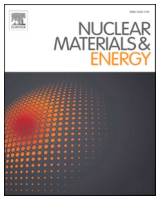

Studies of the formation and distribution of cracks and various defects on the heated tungsten plate surface during pulsed plasma flux impact

M.K. Dosbolayev [a], A.B. Tazhen [a,*], A.N. Kholmirzayev [a], Y.A. Ussenov [b,1], T.S. Ramazanov [a]

[a] Institute of Experimental and Theoretical Physics, Al-Farabi Kazakh National University, Almaty 050040, Kazakhstan
[b] National Nanotechnology Laboratory of Open Type, Al-Farabi Kazakh National University, Almaty 050040, Kazakhstan

ARTICLE INFO

Keywords:
Plasma flux
Pulsed plasma accelerator
Tungsten plate
Ductile–brittle transition temperature
Cracks
Craters

ABSTRACT

In this work, cracking of the surface of a tungsten plate was studied using a PW-7 pulsed plasma accelerator. The surface of the tungsten plate was exposed at an energy density and plasma flux duration of 1.1 MJ/m^2 and 200 μs, respectively. Before each shot, the base of the tungsten plate was heated to a temperature of 823 K. Heating of the base of the tungsten plate above the ductile–brittle transition temperature made it possible to control the temperature gradient on its surface under pulsed plasma exposure. In other words, the temperature gradient of the tungsten plate before and after exposure to the plasma flux decreased. Compared to the data at room temperature, the results of heating of the tungsten plate to the tungsten ductile–brittle transition temperature of 823 K showed a reduction in crack width to several hundred nanometers under the influence of plasma. It should be noted that heating of the plate did not completely eliminate cracking of the surface of the tungsten plate. However, this significantly minimizes the emission of dust from the surface of the tungsten plate under the influence of the plasma flux (barely no dust was observed).

1. Introduction

A detailed understanding of the interaction of the plasma edge region with the first wall in current magnetic plasma confinement facilities is extremely important for improving the overall efficiency of fusion devices. The materials of the first wall can be significantly damaged by highly concentrated energy fluxes escaping from the edge region of the plasma [1–3]. This can be caused by plasma disruptions and edge localized modes (ELM of the order of ~1 MJ/m^2 for ~0.5 ms with a frequency above 1 Hz) [4–5]. For instance, arcing on the surface of ITER-grade tungsten can be detected during tests in the T-10 tokamak [6], and it is mainly observed over the rough surface. Surface roughness is usually caused by the following erosion processes: cracking and melting of the surface layer, movement of the molten layer, and consequent recrystallization [7–9]. When the temperature of unirradiated tungsten exceeds the ductile–brittle transition temperature, it can undergo significant plastic deformation [10]. In this case, the surface of the material risks cracking when cooling. Therefore, a high thermal load and heat flux from the plasma onto the cooled tungsten can lead to its brittle damage. Tungsten tends to exhibit brittle behavior below the ductile-to-brittle transition temperature. It is confirmed by computer simulation, that this transition is the predominant reason for tungsten cracking [11–13]. The temperature limit of the base surface was calculated by numerical analysis under a short-term thermal load of 0.2 GW/m^2 for 0.5 ms in [14] to avoid plastic deformation of tungsten. This temperature limit is in the range of 673–1053 K. Electron and laser beam experiments showed that cracks formed on the surface of the tungsten plate at the cooling stage were caused by plastic deformation in the brittle temperature range between RT and DBTT (~ 673 K) [15–16]. Studies of the characteristics and behavior of tungsten after plasma exposure are attracting increasing attention as they are extremely important for providing safe and highly efficient operation of the reactor. Previous studies on the formation of dust particles in the vicinity of the test tungsten substrate after pulsed plasma exposure showed that the main source of the dust particles is elongated microcracks [17,18]. Results on the tensile strength of a tungsten plate with two different microstructural states heated to a temperature of 573–873 K in an oven are presented in [19]. It is shown, that tungsten plates are susceptible to brittle damage at temperatures below 673 K. The recrystallized microstructure demonstrates more ductile properties at higher temperatures (>673 K) compared to the initial state. Consequently, controlling the temperature of the first wall could minimize surface cracking caused by

* Corresponding author.
E-mail address: Tazhen.Aigerim.B@gmail.com (A.B. Tazhen).
[1] Currently with the Department of MAE, Princeton University, 08540 Princeton, NJ, USA.

https://doi.org/10.1016/j.nme.2023.101540
Received 6 July 2023; Received in revised form 10 October 2023; Accepted 16 October 2023
Available online 18 October 2023

thermal stress. Therefore, irrespective of the type of experiments, the results of these works show that the initial temperature of tungsten plates under deforming stresses is the major factor affecting their subsequent condition.

This work aims to study cracking of a heated tungsten plate after plastic deformation caused by the impact of a pulsed plasma flux.

2. Materials and methods

Experiments to test a tungsten plate were carried out on a PW-7 pulsed plasma installation [20,21] at a certain number of pulses (13, 26, and 39). Pulsed plasma installations provide plasma pulses with a duration of several hundred microseconds, which corresponds to the duration of repetitive ELMs. In addition, they provide not only energy, but also shock loads. In pulsed plasma installations, only the surface layer of the material is heated, so it is possible to study such surface processes as the movement and splashing of molten layers of material, the formation of vapor clouds of the material, etc. The choice of pulse series 13, 26, 39 is justified by comparing this work with the previous work [17]. In this work, the tungsten plate was not only exposed to the plasma flux, but also heated at the same time. The goal of the work was to analyze the state of the surface of the tungsten plate at a given initial temperature. Therefore, to compare the results, the number and cycle of pulses were chosen to be as identical as possible. Moreover, the choice of an odd number of plasma pulses in both works did not depend on the specific experimental conditions.

Before each shot, the tungsten plate is heated to a temperature 823 ± 5 % K above the ductile–brittle transition temperature of tungsten. The temperature of the plate was measured with a Type K thermocouple (chromel–alumel). Before experiments, the residual air is pumped out of the vacuum chamber to a pressure of 10^{-3} Torr. Then the chamber is filled with a plasma-forming gas - hydrogen. The following parameters were maintained for all series of experiments (unless otherwise noted): the capacitor voltage of 4 kV, the gas pressure in the vacuum chamber of 30 mTorr. The main plasma flux parameters are: the diameter ~ 4 cm, the velocity around 27 km/s, the maximum energy density ~ 1.1 MJ/m^2, and the pulse duration about 200 μs. A schematic illustration of the experiment is shown in Fig. 1.

The surface morphology was analyzed using scanning electron microscopy (SEM). The impact of plastic deformation on the crystalline structure of the near-surface layer of the tungsten plate was estimated by X-ray diffraction (XRD) and was carried out on a Rigaku MiniFlex 600 spectrometer. X-ray diffraction of the Kα line of a copper anode was used (accelerating voltage – 40 kV, current – 15 mA). The measuring ranges and steps are 30°-140° and 0.02°, respectively. The composition of the tungsten plate was determined using EDS analysis. The rise in temperature of the tungsten plate surface immediately after exposure to the plasma beam was measured with a conducting thermistor (bolometer) [22]. The bolometer was placed in the same position as the tungsten plate. The main component of the bolometer is a tantalum plate of 40 μm thickness. The active surface area and the initial resistance of the tantalum plate are $2.4 \cdot 10^{-7}$ m^2 and 0.6 Ohm, respectively. A resistor (116.4 Ohm) and a voltage source (6.13 V) were connected in series to the bolometer. At the ends of the resistor, the voltage drop is measured with an oscilloscope. The bolometer heats after the impact of the plasma flux. As a result, the bolometer resistance increases. Consequently, the voltage drop at the ends of the resistor also increases. Since the resistor and the bolometer are connected in series, the voltage drop across the resistor increases in the same way as the voltage drop across the bolometer plate. The use of standard formulas and calculations allows us to evaluate the resistance changes of the bolometer. The temperature of the tantalum plate is calculated using the formula (1). The temperature distribution plot is shown in Fig. 2.

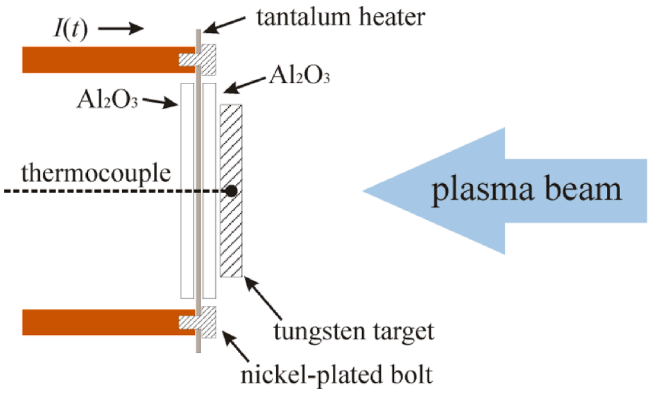

Fig. 1. Schematic illustration of the experiment.

$$\Delta T = T_2 - T_1 = \frac{R_2 - R_1}{\alpha \cdot R_1}, \quad (1)$$

where T_1, R_1, and T_2, R_2 are the temperature and resistance of the bolometer before and during exposure to the plasma flux, $\alpha = 0,0031 K^{-1}$ is the tantalum temperature coefficient. The temperature of the bolometer plate at the initial moment of time (<60 μs) could not be measured, as shown in Fig. 2a, since the flux of energetic plasma created strong electrical noise caused by a direct contact of the tantalum plate with the plasma flux. As mentioned above, the tantalum plate is quite thin. Therefore, it instantly heats up under the influence of the plasma flux, and also cools down quickly, since it is installed on massive conductors. Thus, we estimate that the surface of the tungsten plate is also strongly heated to a temperature of 4500 K under the influence of the plasma flux.

The time dependence of the energy density of the plasma flux was measured. For this purpose, a cone-shaped calorimeter was made of 200 μm thin titanium foil. The surface area of the calorimeter onto which the plasma flux falls is 16.8 cm^2. K-type thermocouples were attached to the outer wall of the calorimeter (on the back side of the plasma flux). The enhanced thermo electromotive force (EMF) at the ends of the thermocouple was recorded by a storage oscilloscope through a low-pass filter. Thus, the energy density of the plasma flux at the peak approached 1.1 MJ/m^2 (Fig. 2b), which corresponds to the thermal loads in the edge localized mode (ELM) of ITER. The plasma flux velocity can be estimated from Fig. 2b. The plasma flux reached the calorimeter within a time of 8 μs from the point where the interelectrode plasma jumper appeared (corresponds to the noise in Fig. 2b). The distance is 24 cm. In this case, the plasma flux velocity is at least 30 km/s.

3. Preparation of samples

For all experiments, commercially available rolled polycrystalline tungsten (99.96 %) was used (Fig. 3). Tungsten plate size: thickness is 2 mm, width and height are 15 mm. The surface was subjected to uniform plasma exposure, since the dimensions of the tungsten plate are significantly smaller than the diameter of the plasma flux and it was located in the central part of the beam. The substrates were first subjected to sequential wet grinding with 800 to 2500 grit abrasive paper (5 min per sample on each abrasive paper), and then the plate was electrochemically polished in a weak solvent (KOH). After this, the plates were washed in alcohol and deionized water to remove all possible residual impurities and contaminants.

4. Results and discussion

After continuous exposure to 13 plasma pulses, SEM analysis of the sample revealed the presence of spots of different sizes on the surface of the tungsten plate (Fig. 4a). After EDS analysis (Fig. 5c), it was shown that these spots contain nickel impurities. Note that the initial surface composition of the tungsten plate consisted exclusively of tungsten

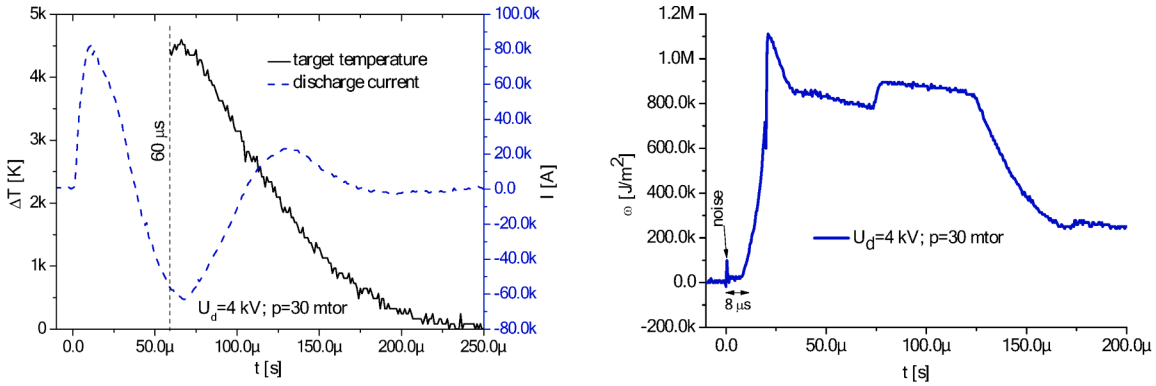

a) Temperature evolution of a bolometer under the influence of a plasma flux. The oscillogram of the discharge current is highlighted with a dashed line

b) Time dependence of the energy density of plasma flux

Fig. 2. Main parameters of the PW-7 pulsed plasma accelerator.

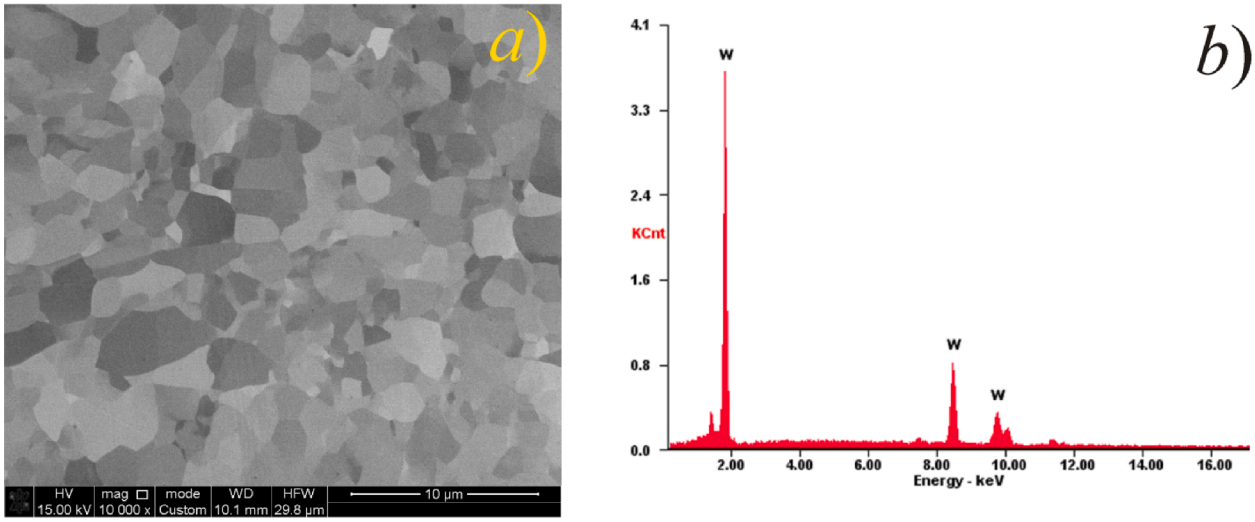

Fig. 3. *a*) Smooth surface of a tungsten plate after electromechanical polishing, *b*) elemental composition of a tungsten plate according to EDS analysis.

(Fig. 3b). However, the presence of nickel impurities led to a change in the surface morphology (Fig. 4a-4d). These impurities, likely caused by the mounting screws used to secure the housing heating elements, formed thin films on the surface of the tungsten plate. The intense sputtering of these screws occurred due to overheating caused by the plasma flux.

Changes in spots on the surface were observed after a certain number of pulses. SEM analysis of spots after 13, 26, and 39 pulses is shown in Fig. 4c, 5a, and 5b, respectively. In these spots, cracks were found that were wider than the other observed cracks (Fig. 4d). In addition, blisters were found in places where nickel impurities accumulated, as shown by the white arrows in Fig. 5a.

As reported in [23–25], the deposition of films on the surface significantly enhances the blistering process. Hydrogen can diffuse between the thin film and the surface of the material due to thermal stress. During this process, hydrogen gas molecules accumulate, which subsequently leads to the formation of blisters (Fig. 5a, shown by white arrows). Nickel is not used as a tokamak material. However, the results of these studies show that the integration of foreign element impurities on the surface of the tungsten plate can cause an increased likelihood of defects such as blisters. We suppose that the presence of foreign material on the tungsten surface does not adhere properly, making it more susceptible to peeling. On the other hand, nickel (~28 eV) has a lower threshold bias energy than tungsten (90 eV) [26].This increases the probability of hydrogen implantation and the formation of an internal hydrogen molecular cavity. Thus, with repeated exposure to the plasma flux, the temperature (pressure) of the gas between the layers increases, which leads to the formation of bubbles.

After 26 pulses, the blister caps open and peel off. This is due to an increase in the temperature of local surface areas, especially areas with cracks. The appearance of cracks deteriorates the properties of the tungsten plate and, perhaps, reduces its thermal conductivity. In this case, most of the absorbed energy of the plasma flux is used to heat the edges of the cracks, and not propagate into depth (Fig. 5a, indicated by

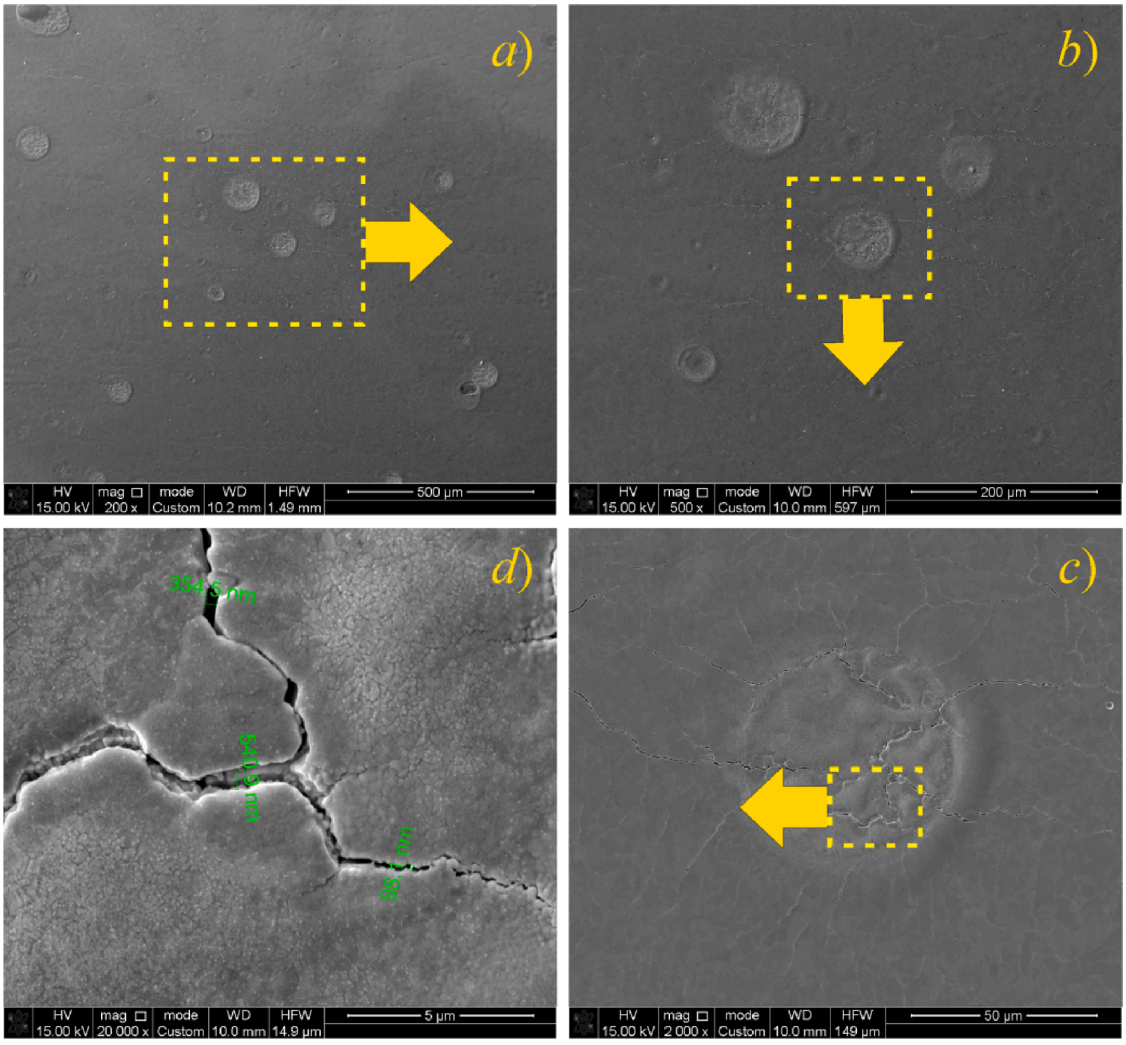

Fig. 4. The surface of a tungsten plate after a 13-pulse exposure to a plasma flux. Dashed boxes indicate enlarged images.

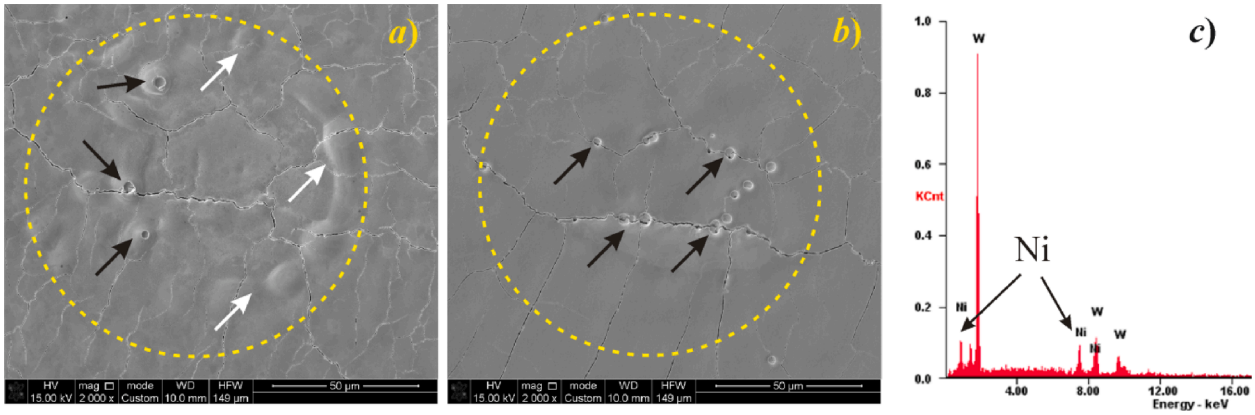

Fig. 5. The surface of a tungsten plate after exposure to 26 (*a*) and 39 (*b*) pulses. Elemental composition of the plate with spots obtained by the EDS method (*c*).

black arrows).

Traces of craters were observed in the vicinity of the crack (Fig. 5b, marked with black arrows). The craters appeared as a result of the action of a unipolar arc on the sharp edges of cracks. Numerous studies have been conducted to study the effect of plasma thermal shock on the microstructure of tungsten [27,28], and they showed that structural damage (the occurrence of mechanical stress) is the main cause of cracking. This poses a serious problem for such projects as ITER and DEMO. Previous studies [29,30] have shown that tungsten plates experience thermal expansion in the plasma load region. However, the cold and unloaded area of the plate resists such expansion. Consequently, compressive plastic deformation occurs in the material. Compressive stresses significantly decrease during the periods of cooling of the tungsten plate. In this case, tensile plastic deformations occur

(ductile–brittle transition). Tensile plastic deformations cannot completely compensate for compressive plastic deformations. As the authors report [14–16], during thermo plasma exposure, the behavior of tungsten strongly depends on its temperature. In particular, this work focuses on the influence of base temperature on crack behavior. A positive effect was found: as follows from the results, when the plate is heated to a temperature above the tungsten ductile–brittle transition temperature (>673 K), cracking of the plate is practically not expected.

In tungsten samples without preheating, cracks with a size of about 7–10 μm were observed, which were reported in [17]. In the current experiments, the tungsten plate was preheated before being exposed to the plasma pulse. The crack width was reduced to several hundred nanometers by heating the plate to a temperature of 823 K (Fig. 6a-6b), and the maximum observed crack width was 315 nm.

The development of cracks on the surface of the plate was studied by the number of applied pulses. After increasing the number of pulses from 13 to 26 and 39, respectively, the development of cracks and expansions was negligible. The cracks changed orientation during the expansion and modification process (Fig. 6c and 6d, Fig. 6e and 6f), compared to the previous work [17]. This may be due to the redistribution of thermal stresses in the material after a series of plasma impacts.

The area occupied by micro cracks was determined using the ImageJ program. For this purpose, SEM images of the tungsten plate obtained after three plasma exposures were used. Although the statistics is small, relatively accurate results were obtained. The area of cracks on a unit surface of a tungsten plate after exposure to 13 plasma pulses was 7.4 μm^2. This corresponds to approximately 1 % of the total surface area of the plate. The crack area after 26 pulses was 12 μm^2 (1.6 %) and after 39 pulses 11.65 μm^2 (1.56 %), respectively.

SEM images of the cross section of the tungsten plate obtained after 39 pulses are shown in Fig. 7.

In this case, frequently repeated images of micro cracks were selected. The cracks grew with slight tortuosity perpendicular to the surface, without branching. A study of the cross section of the plate showed some specific features. For example, the crack in Fig. 7a with a depth of 3.9 μm could have appeared after one of the last plasma pulses. This conclusion was based on the fact that the crack was not modified and had a large width of about 320 nm. Cracks consisting of several deep channels were also observed (Fig. 7b and 7c). Deep longitudinal channels that do not extend to the surface of the plate are traces of primary cracks. Fig. 7d clearly shows how one of these channels closed (the upper part of the crack to a depth of 2.3 μm). According to our considerations, this effect may be caused by subsequent plasma pulses, during which the surface of the tungsten plate is remelted.

Thermal stresses generated in the tungsten plate are the main cause of surface cracking and are limited mainly to the near-surface layer of tungsten (under short-term loading).

The magnitude of thermal stress was estimated using diffraction-based measurements [31]:

$$\sigma = E \cdot \frac{\Delta d}{d} \tag{2}$$

where E is Young's modulus, d is the distance between crystallographic planes without stress, Δd is the difference between the distances between crystallographic planes with and without stresses. To achieve accuracy, the diffraction line (321) located in the region of the exact angle ($\theta > 60^0$) was used (Fig. 8d). The shift of the diffraction line towards larger angles indicates a decrease in the distance (d) between the reflecting crystallographic planes. Therefore, it can be concluded that compressive stress occurs in this case. The calculated d values of unstressed and stressed tungsten are 0.08235 and 0.08232 nm. The corresponding value of $\Delta d/d$ is 0.000364. The compressive stress in the tungsten plate, calculated by formula (2) is equal to 125.6 MPa. The shift of the diffraction line was determined from the analysis of the graph in Fig. 8d.

After exposure to the plasma flux, the broadening of the diffraction lines was observed, which indicates a high dislocation density in the surface layer of the heated tungsten plate (Fig. 8b-8d). Interestingly, increasing the number of pulses from 13 to 26 and then to 39 did not significantly change the thermal stresses. Hence, the results show that the occurrence of cracks can be effectively controlled by preheating of the tungsten plate, which can potentially effectively eliminate their

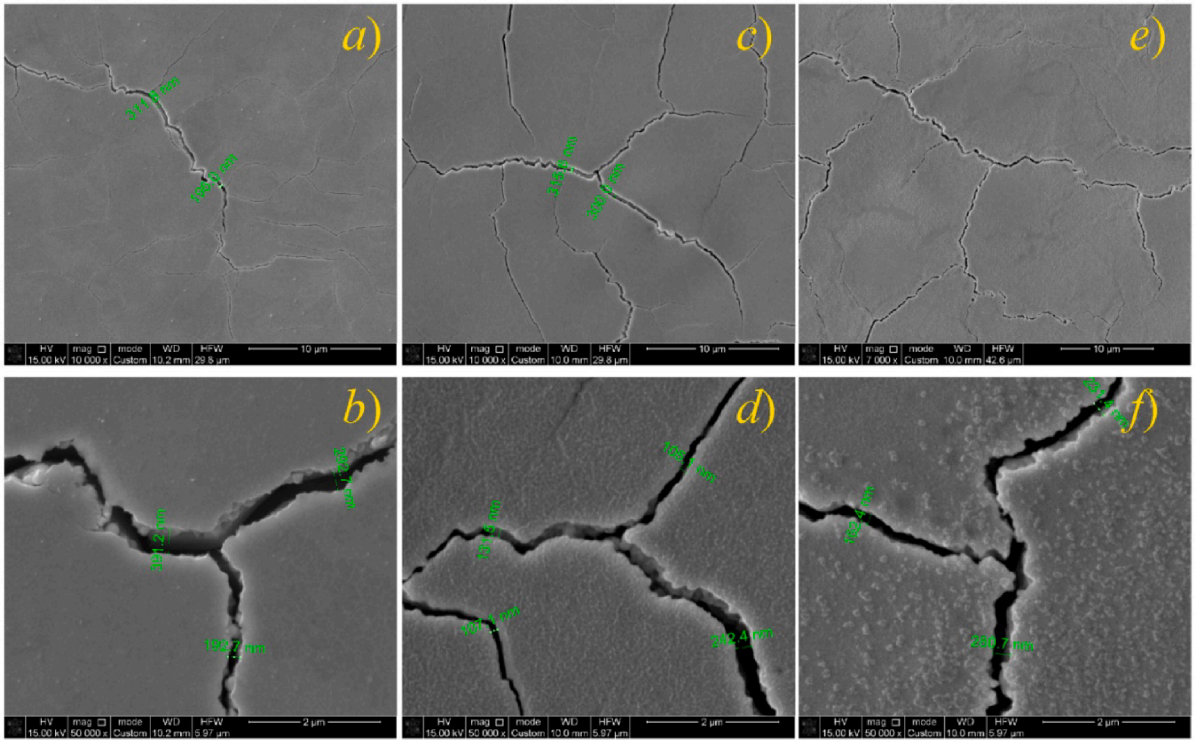

Fig. 6. The surface of a tungsten plate after 13 pulses (*a* and *b*), 26 pulses (*c* and *d*), and 39 pulses (*e* and *f*).

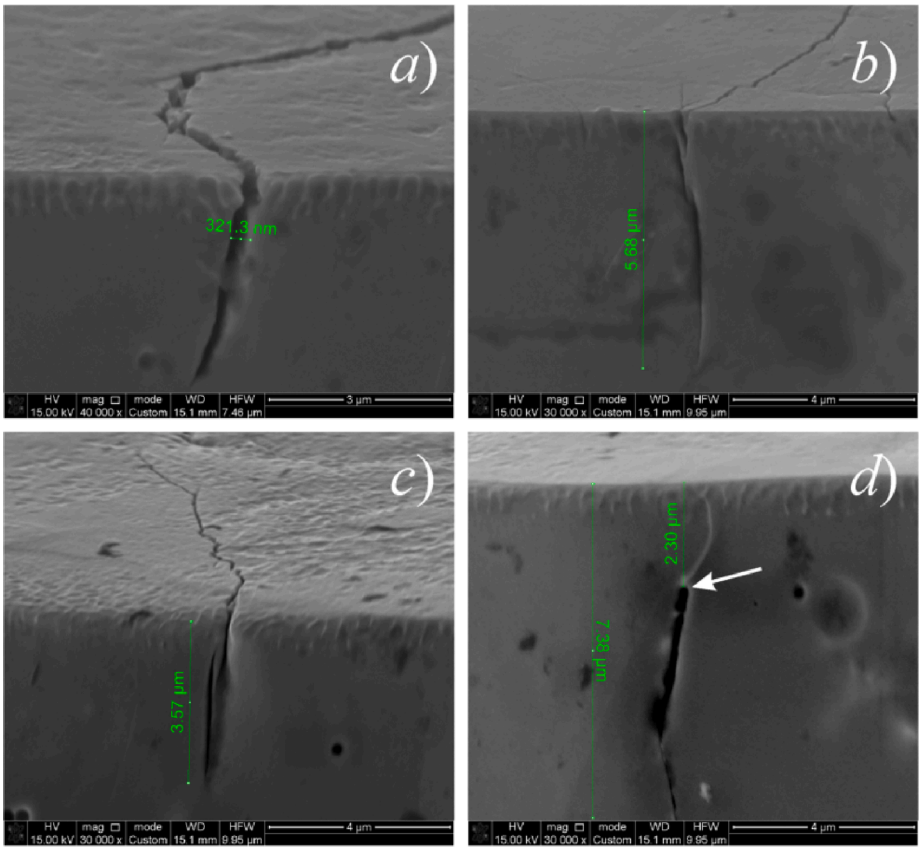

Fig. 7. Cross section of a tungsten plate after exposure to 39 pulses.

negative effects. Preheating allows us to control the temperature gradient of the plate surface before and after exposure to a pulsed plasma flux. As the results of our previous studies show [17], when exposed to plasma, large cracks maintain their position and only increase due to splitting and melting of sharp edges. Ejected tungsten particles can also melt even below the melting threshold at low thermal loads. This may be the main reason for the formation of dust droplets, Fig. 9a and 9b.

It was found that the effect of plasma flux on preheated tungsten plates does not lead to the potential formation of dust particles and droplets (Fig. 9c and 9d). Unlike the previous work where the formation of tungsten dust was caused by cracks, no significant cracking was observed in this case. Hence, dust generation was significantly reduced, providing a favorable result in terms of dust generation. Exposure to the plasma flux does not lead to potential dust formation in preheated tungsten plates (Fig. 9c and 9d).

The tungsten dust in the previous work was caused by cracks. However, in this case, no significant cracking was observed. This made it possible to reduce dust formation significantly. The interaction of the plasma flux with the material was recorded by a Phantom VEO710S high-speed camera. The recording speed was 20,000 frames per second.

The micron-sized arc craters, similar to those identified on the T-10 Tokamak [32], were formed (Fig. 10). These craters predominantly arise from a unipolar arc process occurring between the solid target and the plasma [33]. As mentioned earlier, a rough surface is one of the main factors in the occurrence of unipolar arcs. At the same time, surface defects of the tungsten plate, including cracks, noticeably increase the surface roughness, thereby increasing the likelihood of arc crater formation.

As reported in [34], unipolar arcs on surfaces are one of the dominant mechanisms of plasma erosion of the metal surface. They lead to the following effects: overheating of the surface, local melting, and increased emission of electrons into the plasma from the surface. Unfortunately, there is currently no suitable diagnostic equipment to study the speed and other important characteristics of the arc. As reported in [35], the main factor influencing the formation of micro craters by unipolar arcs is explosive electron emission. As shown in Fig. 10a-10f, such craters have an approximately hemispherical shape.

5. Conclusion

The behavior of a preheated tungsten plate after exposure to a plasma flux was investigated at the PW-7 pulsed plasma accelerator. Preheating of the tungsten plate resulted in a significant reduction in thermal stress values compared to the previous experiments in which no preheating was used. This suggests that preheating plays a crucial role in reducing thermal stress and its harmful effects on the tungsten plate. It has been noted, that the thermal stress does not change significantly and practically relaxes with an increase in the number of pulses from 13 to 26 and to 39. After exposure to the plasma flux, defects such as cracks and arc craters were detected, which indicates macroscopic erosion. Reducing the temperature gradient of the surface of the tungsten plate (candidate material) before and after plasma exposure by 823 K allowed us to avoid the appearance of cracks with a width of more than 1 µm, which is in good agreement with the results of the other authors [13–16]. Moreover, in this case, dust formation under the influence of a plasma flux is significantly reduced. In addition to cracks, arc craters, and blisters were found on the surface of the tungsten plate. Such surface defects are apparently caused by the process of arc formation on a rough surface.

However, degradation of the surface of the tungsten plate under the action of cyclic plasma pulses remains a topic for further investigation. It is important to note that while preheating can reduce surface cracking, it cannot eliminate it. Therefore, comprehensive investigation focusing on

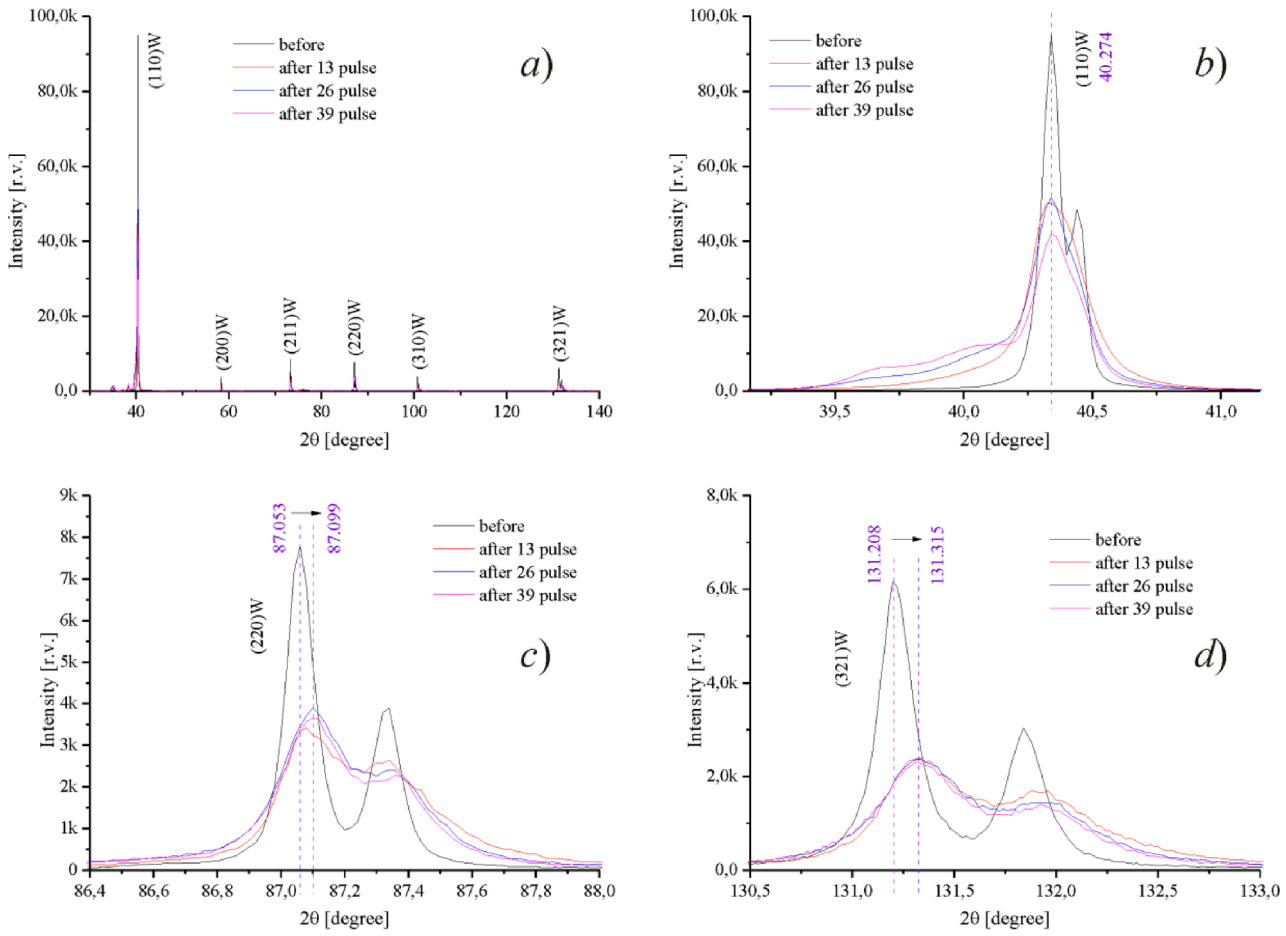

Fig. 8. Results of X-ray diffraction analysis: *a*) general spectra, *b*) angle 40.274, *c*) angle 87.053, *d*) angle 131.208.

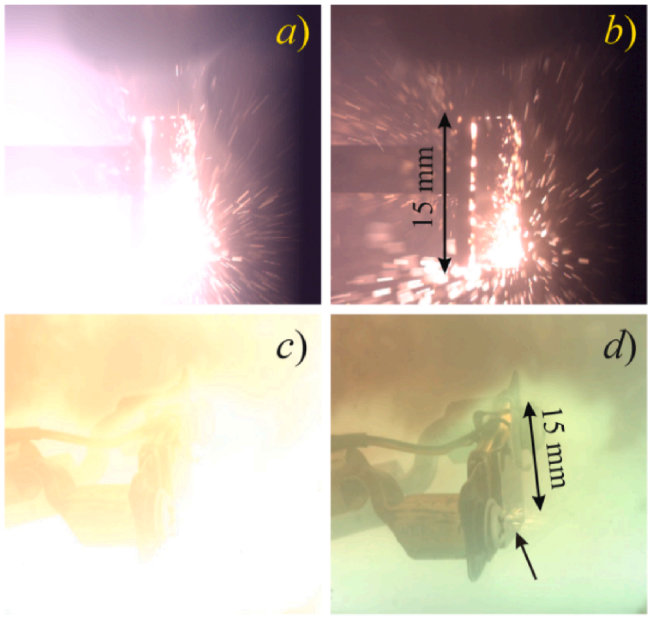

Fig. 9. Photographs of erosion of the surface of a tungsten plate: during (a [11] and c) and after (b [11] and d) exposure to a plasma flux. The plasma beam is directed from right to left perpendicular to the surface of the tungsten plate (15x15 mm).

various aspects such as surface roughness, crack width, crack depth, and crack spacing is still needed to gain a deeper understanding of surface degradation and its characteristics under these conditions. This comprehensive study will provide valuable information that will enable scientists to improve the durability and performance of tungsten plates in similar plasma environments of modern fusion devices such as ITER and DEMO.

Funding

This work was supported by the Ministry of Science and Higher Education of the Republic of Kazakhstan (project no. IRN AP09259081).

CRediT authorship contribution statement

M.K. Dosbolayev: Conceptualization, Methodology, Investigation, Writing – original draft. **A.B. Tazhen:** Conceptualization, Methodology, Data curation, Investigation, Writing – original draft. **A.N. Kholmirzayev:** Conceptualization, Methodology, Data curation, Investigation, Writing – original draft. **Y.A. Ussenov:** Writing – review & editing. **T.S. Ramazanov:** Investigation, Supervision, Writing – review & editing.

Declaration of Competing Interest

The authors declare that they have no known competing financial interests or personal relationships that could have appeared to influence the work reported in this paper.

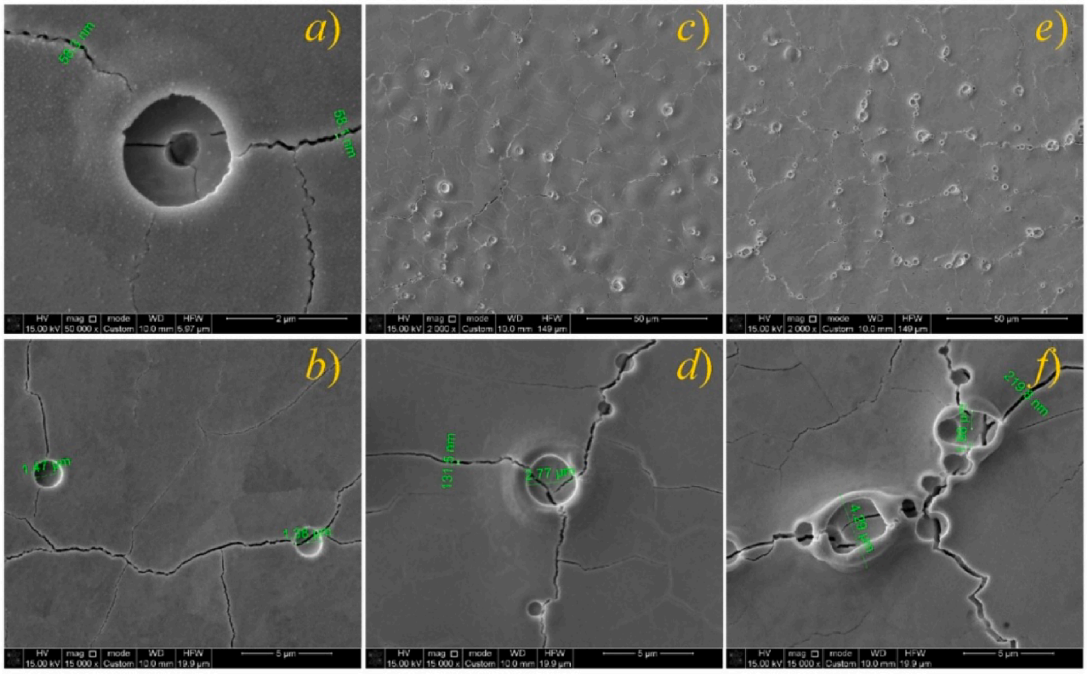

Fig. 10. Arc craters on the surface of a tungsten plate after: 13 pulses (*a* and *b*), 26 pulses (c and *d*), and 39 pulses (*e* and *f*).

Data availability

Data will be made available on request.

References

[1] J. Linke, J. Du, T.h. Loewenhoff, G. Pintsuk, B. Spilker, I. Steudel, M. Wirtz, Challenges for plasma-facing components in nuclear fusion, Matter Radiat. Extremes 4 (2019), 056201, https://doi.org/10.1063/1.5090100.

[2] G.L. Xu, J. Guterl, T. Abrams, H.Q. Wang, J.D. Elder, E.A. Unterberg, D.M. Thomas, P.C. Stangeby, H.Y. Guo, M.Y. Ye, Modeling of inter- and intra-edge-localized mode tungsten erosion during DIII-D H-mode discharges, Nucl. Fusion 59 (2019), 126018, https://doi.org/10.1088/1741-4326/ab3e96.

[3] M. Reinhart, S. Brezinsek, A. Kirschner, J.W. Coenen, T. Schwarz-Selinger, K. Schmid, A. Hakola, H. van der Meiden, R. Dejarnac, E. Tsitrone, Latest results of Eurofusion plasma-facing components research in the areas of power loading, material erosion and fuel retention, Nucl. Fusion 62 (2022), 042013, https://doi.org/10.1088/1741-4326/ac2a6a.

[4] J. Linke, T. Hirai, M. Rödig, L. Singheiser, Performance of plasma-facing materials under intense thermal loads in tokamaks and stellarators, Fus. Sci. Technol. 46 (2004) 142. 10.13182/FST04-A550.

[5] T. Hirai, K. Ezato, P. Majerus, ITER Relevant High Heat Flux Testing on Plasma Facing Surfaces, Mater. Trans. 46 (3) (2005) 412–424, https://doi.org/10.2320/matertrans.46.412.

[6] V.P. Budaev, S.A. Grashin, A.V. Karpov, L.N. Khimchenko, Role of arc formation in overheating of tungsten limiter in the T-10 tokamak at high heat loads expected in the ITER tokamak, J. Phys. Conf. Ser. 1094 (2018), 012006, https://doi.org/10.1088/1742-6596/1094/1/012006.

[7] I. Bykov, C.P. Chrobak, T. Abrams, D.L. Rudakov, E.A. Unterberg, W.R. Wampler, E.M. Hollmann, R.A. Moyer, J.A. Boedo, B. Stahl, Tungsten erosion by unipolar arcing in DIII-D, Phys. Scr. T170 (2017), 014034, https://doi.org/10.1088/1402-4896/aa8e34.

[8] L.N. Vyacheslavov, A.A. Vasilyev, A.S. Arakcheev, D.E. Cherepanov, I. V. Kandaurov, A.A. Kasatov, V.A. Popov, A.A. Ruktuev, A.V. Burdakov, G. G. Lazareva, A.G. Maksimova, A.A. Shoshin, In-situ study of the processes of damage to the tungsten surface under transient heat loads possible in ITER, J. Nucl. Mater. 544 (2021), 152669, https://doi.org/10.1016/j.jnucmat.2020.152669.

[9] G. Sinclair, J.K. Tripathi, P.K. Diwakar, A. Hassanein, Melt layer erosion during ELM-like heat loading on molybdenum as an alternative plasma-facing material, Sci. Rep. 7 (1) (2017) 12273, https://doi.org/10.1038/s41598-017-12418-z.

[10] Y. Oh, W.-S. Ko, N. Kwak, T. Jae-il Jang, H.N.H. Ohmura, Small-scale analysis of brittle-to-ductile transition behavior in pure tungsten, J. Mater. Sci. Technol. 105 (2022) 242–258, https://doi.org/10.1016/j.jmst.2021.07.024.

[11] Sh.Wang, J. Li, Ye Wang, X. Zhang, R. Wang, Y. Wang, J. Cao, Thermal damage of tungsten-armored plasma-facing components under high heat flux loads, Sci Rep. 10 (2020) 1359, 10.1038/s41598-020-57852-8.

[12] S.-M. Wang, J.-S. Li, Y.-X. Wang, X.-F. Zhang, Q. Ye, Thermal Shock Behavior Analysis of Tungsten-Armored Plasma-Facing Components for Future Fusion Reactor, Acta Metallurgica Sinica (English Letters) 3 (2018) 515–522, https://doi.org/10.1007/s40195-018-0721-9.

[13] L. Changjun, Z.h. Dahuan, L. Xiangbin, W. Baoguo, C.h. Junling, Thermal-stress analysis on the crack formation of tungsten during fusion relevant transient heat loads, Nuclear Materials and Energy 000 (2017) 1–6, https://doi.org/10.1016/j.nme.2017.06.008.

[14] T. Hirai, G. Pintsuk, Thermo-mechanical calculations on operation temperature limits of tungsten as plasma facing material, Fusion Eng. Des. 82 (2007) 389–393. https://doi:10.1016/j.fusengdes.2007.03.032.

[15] T. Hirai, G. Pintsuk, J. Linke, M. Batilliot, Cracking failure study of ITER-reference tungsten grade under single pulse thermal shock loads at elevated temperatures, J. Nucl. Mater. 390–391 (2009) 751–754. https://doi:10.1016/j.jnucmat.2009.01.313.

[16] A. Huber, A. Arakcheev, G. Sergienko, I. Steudel, M. Wirtz, A.V. Burdakov, J. W. Coenen, A. Kreter, J. Linke, P.h. Mertens, V. Philipps, G. Pintsuk, M. Reinhart, U. Samm, A. Shoshin, B. Schweer, B. Unterberg, M. Zlobinski, Investigation of the impact of transient heat loads applied by laser irradiation on ITER-grade tungsten, Phys. Scr. 159 (2014), 014005. https://doi:10.1088/0031-8949/2014/T159/014005.

[17] M.K. Dosbolayev, A.B. Tazhen, T.S. Ramazanov, Ye.A. Ussenov, Investigation of dust formation during changes in the structural and surface properties of plasma-irradiated materials, Nucl. Mater. Energy 33 (2022) 101300, 10.1016/j.nme.2022.101300.

[18] V.A. Makhlaj, I.E. Garkusha, N.N. Aksenov, A.A. Chuvilo, V.V. Chebotarev, I. Landman, S.V. Malykhin, S. Pestchanyi, A.T. Pugachov, Dust generation mechanisms under powerful plasma impacts to the tungsten surfaces in ITER ELM simulation experiments, J. Nucl. Mater. 438 (2013) S233-S236, 10.1016/j.jnucmat.2013.01.034.

[19] V. Shah, J.A.W. van Dommelen, E. Altstadt, A. Das, M.G.D. Geers, Brittle-ductile transition temperature of recrystallized tungsten following exposure to fusion relevant cyclic high heat load, J. Nucl. Mater. 541 (2020), 152416, https://doi.org/10.1016/j.jnucmat.2020.152416.

[20] A.B. Tazhen, Z.R. Rayimkhanov, M.K. Dosbolayev, T.S. Ramazanov, Generation and Diagnostics of Pulse Plasma Flows, Plasma Phys. Rep. 46 (2020) 465–471, https://doi.org/10.1134/S1063780X20040121.

[21] M.K. Dosbolayev, A.B. Tazhen, T.S. Ramazanov, Investigation and diagnostics of plasma flows in a pulsed plasma accelerator for experimental modeling of processes in tokamaks, Eurasian J. Phys. Functional Mater. 5 (2021) 198–210. 10.32523/ejpfm.2021050404.

[22] M.K. Dosbolayev, A.U. Utegenov, A.B. Tazhen, T.S. Ramazanov, Investigation of dust formation in fusion reactors by pulsed plasma accelerator, Laser Part. Beams 35 (4) (2017) 741–749, https://doi.org/10.1017/S0263034617000805.

[23] Y. Ueda, M. Fukumoto, I. Sawamura, D. Sakizono, T. Shimada, M. Nishikawa, Carbon impurity behavior on plasma facing surface of tungsten, Fusion Eng. Des. 81 (2006) 233–239, https://doi.org/10.1016/j.fusengdes.2005.08.047.

[24] X.-X. Zhang, L. Qiao, H. Zhang, Y.-H. Li, P. Wang, C.-S. Liu, Surface blistering and deuterium retention behaviors in pure and ZrC-doped tungsten exposed to deuterium plasma, Nucl. Fusion 61 (2021), 046026, https://doi.org/10.1088/1741-4326/abdfda.

[25] L.B. Begrambekov et al, Behaviour of Redeposited Tungsten Layers with Varying Impurity Content during Thermal and Radiation Loads, J. Phys.: Conf. Ser. 1238 (2019) 012001, 10.1088/1742-6596/1238/1/012001.
[26] M.J. Banisalman, S. Park, T. Oda, Evaluation of the threshold displacement energy in tungsten by molecular dynamics calculations, J. Nucl. Mater. 495 (2017) 277–284, https://doi.org/10.1016/j.jnucmat.2017.08.019.
[27] H. Sattar, Sh. Jielin, H. Ran, M. Imran, W. Ding, P. Das Gupta, H. Ding, Impact of microstructural properties on the hardness of tungsten heavy alloy evaluated by stand-off LIBS after PSI plasma irradiation, J. Nucl. Mater. 540 (2020) 152389, 10.1016/j.jnucmat.2020.152389.
[28] I.E. Garkusha, V.A. Makhlaj, N.N. Aksenov, O.V. Byrka, S.V. Malykhin, A. T. Pugachov, B. Bazylev, I. Landman, G. Pinsuk, J. Linke, M. Wirtz, M.J. Sadowski, E. Skladnik-Sadowska, High power plasma interaction with tungsten grades in ITER relevant conditions, J. Phys. Conf. Ser. 591 (2015), 012030, https://doi.org/10.1088/1742-6596/591/1/012030.
[29] M. Li, E. Werner, J.-H. You, Cracking behavior of tungsten armor under ELM-like thermal shock loads: A computational study, Nuclear Materials & Energy 2 (2015) 1–11, https://doi.org/10.1016/j.nme.2014.10.001.
[30] B. Vrancken, R.K. Ganeriwala, A.A. Martin, M.J. Matthews, Microcrack mitigation during laser scanning of tungsten via preheating and alloying strategies, Addit. Manuf. 46 (2021), 102158, https://doi.org/10.1016/j.addma.2021.102158.
[31] M. Bhuyan, S.R. Mohanty, C.V.S. Rao, P.A. Rayjada, P.M. Raole, Plasma focus assisted damage studies on tungsten, Appl. Surf. Sci. 264 (2013) 674–680, https://doi.org/10.1016/j.apsusc.2012.10.093.
[32] V.P. Budaev, L.N. Khimchenko, S.A. Grashin, A.V. Karpov, Arcing effects on tokamak first wall tungsten components exposed to plasma loads, VANT. Ser. Fusion 42 (2019) 51–56. 10.21517/0202-3822-2019-42-1-51-56.
[33] B. Wang, D. Zhu, R. Ding, B. Gao, R. Yan, C.h. Li, C.h. Xuan, B. Yu, J. Chen, Observations on arcing on the metal plasma-facing components in EAST, Nuclear Materials & Energy 34 (2023), 101318, https://doi.org/10.1016/j.nme.2022.101318.
[34] D.L. Rudakov, C.P. Chrobak, R.P. Doerner, S.I. Krasheninnikov, R.A. Moyer, K.R. Umstadter, W.R. Wampler, C.P.C. Wong, Arcing and its role in PFC erosion and dust production in DIII-D, J. Nucl. Mater. 438 (2013) S805-S808, 10.1016/j.jnucmat.2013.01.173.
[35] S.A. Barengolts, G.A. Mesyats, M.M. Tsventoukh, The ecton mechanism of unipolar arcing in magnetic confinement fusion devices, Nucl. Fusion 50 (2010) 12500, https://doi.org/10.1088/0029-5515/50/12/125004.